Advances in Science and Technology Research Journal

Advances in Science and Technology Research Journal, 2026, 20(5), 293–311
https://doi.org/10.12913/22998624/216450
ISSN 2299-8624, License CC-BY 4.0

Received: 2025.12.20
Accepted: 2026.03.15
Published: 2026.04.01

Longitudinal vibration analysis of non-uniform rods of any shapes based on differential transforms

Davit Ghazaryan[1], Armine Avetisyan[2*]

[1] College of Science and Engineering, American University of Armenia, 40 Marshal Baghramyan Ave., 0019, Yerevan, Republic of Armenia
[2] Research Laboratory of Automation and Electromagnetic Systems, National Polytechnic University of Armenia, 105 Teryan, 0009, Yerevan, Republic of Armenia
* Corresponding author's e-mail: arm.avetisyan@seua.am

ABSTRACT

A differential transforms based computational method is developed for the free longitudinal vibration analysis of non-uniform rods with smoothly varying cross-sections. The objective is to obtain a numerically stable formulation that accommodates changes in the cross-sectional profile without problem-specific re-derivation. Assuming the area variation is described by a differentiable function $A(x)$, the governing variable-coefficient eigenvalue problem is mapped into the transform domain and expressed through recurrence relations, from which a characteristic polynomial in the frequency parameter is constructed to determine the natural frequencies. The required geometric input is provided solely through the differential spectrum of $A(x)$. The method is validated against a broad set of benchmark problems from the literature, including polynomial, trigonometric, and exponential cross-sectional variations, and reproduces reference eigenfrequencies with agreement up to at least five significant digits, while requiring significantly fewer degrees of freedom than finite element discretizations for comparable accuracy. In addition, the formulation resolves previously reported inconsistencies and yields physically consistent fundamental modes across the examined boundary configurations. The approach is further demonstrated on composite cross-sectional variations beyond standard benchmark profiles.

Keywords: non-uniform rod, longitudinal vibration, differential transforms, vibration analysis.

INTRODUCTION

The longitudinal vibration of rods is one of the most fundamental problems in elastic dynamics. The traveling waves associated with such systems, which can be regarded as elastic waveguides, are non-dispersive, and their importance arises both from their mathematical simplicity and from their role as benchmark problems for more complex scenarios involving variable geometry and boundary conditions. However, many practical engineering structures deviate from this idealization, as their cross-sections are non-uniform and the area is prescribed by a given differentiable function. In such cases, the governing equations of motion contain spatially varying coefficients, which significantly complicates the analytical and numerical treatment of the problem.

The present study addresses this class of problems by employing the differential transform method (DTM) as a unified computational framework for longitudinal vibration analysis. The motivation for adopting this approach lies in the ability of differential transforms to generate recurrent algebraic relations, which can be efficiently handled through inverse transforms. As a result, variable coefficients arising from arbitrary differentiable cross-sectional variations can be incorporated without case-dependent reformulation.

The vibration of non-uniform rods and beams has been extensively investigated in the literature. Abrate [1] provided a comprehensive overview of vibration problems involving non-uniform structural elements. Exact solutions for elastic rods with cross-sectional areas of the form $A(x)=(ax+b)^n$ and $A(x)=\sin^2(ax+b)$ where a and b are real constants and n is an integer, were presented in [2], where x denotes the position along the length of an elastic rod. Closed-form solutions for inhomogeneous rods were developed in [3] for a cross-sectional area $A(x)=kx^n\exp(bx^2)$. In [4], non-uniform rods with cross-sectional area $A(x)=A_0\exp(bx^2)$ where A_0 and b are constants, were analyzed. It should be emphasized that the cross-sectional profiles considered in these studies are largely restricted to specific functional forms that permit analytical tractability

In addition to analytical and semi-analytical techniques, the finite element method (FEM) has been widely employed for the vibration analysis of rods and beams with spatially varying properties. FEM-based formulations can naturally accommodate complex geometries, variable material properties, and discontinuities, and therefore represent a versatile and well-established numerical benchmark for eigenvalue problems with variable coefficients [5–7]. However, FEM solutions generally require fine spatial discretization to accurately predict higher vibration modes, leading to large system matrices and increased computational cost. Furthermore, FEM offers limited analytical insight into the influence of cross-sectional variation on spectral properties and is less efficient for parametric studies involving repeated changes of $A(x)$. Consequently, while FEM serves as a reliable reference solution, there remains a clear demand for semi-analytical approaches that combine generality with low computational cost and explicit control over numerical stability and convergence. This gap motivates the present differential transforms based formulation, which complements FEM by providing a compact and geometry-invariant computational framework for smoothly varying cross-sectional profiles.

Within this context, the DTM is adopted as the primary mathematical tool in the present study. Differential transforms were originally introduced by Pukhov [8] in 1976 for solving differential equations and were later applied to electrical circuit analysis [9]. Subsequently, a series of monographs [10–12] systematically developed the theoretical foundations and operational rules of the method. A review of the differential transform method in modern science was presented in [13]; however, several important contributions were not included, notably those of Simonyan and Avetisyan [14], where invariants of non-autonomous matrices (including eigenvalues, determinants, inverses, and pseudo-inverses) and solutions of linear and nonlinear non-autonomous systems were investigated. Applications to optimal control problems and non-autonomous matrix equations were reported in [15, 16].

The applicability of the differential transforms to vibration analysis has been demonstrated in numerous studies. Suddoung [17] applied the method to the vibration analysis of stepped beams with elastically constrained ends. In [18, 19], it was used for the nonlocal vibration analysis of functionally graded nanobeams and for the vibration analysis of spinning exponentially functionally graded Timoshenko beams. Free vibrations of non-uniform and axially functionally graded Euler–Bernoulli beams were investigated in [20], while a non-uniform rotating Euler–Bernoulli beam was analyzed in [21]. Differential transforms were also employed to study cylindrical shells with cutouts [22], nonlinear time-fractional diffusion equations [23], axially loaded Timoshenko shafts with overhung disks [24], buried pipelines and piles [25], and multi-variable biological systems [26]. In [27], the method was applied to determine the free vibration characteristics of wind turbines with variable cross-sections modeled as equivalent continuous beams.

These studies demonstrate that the DTM provides a computationally stable and versatile tool for solving linear differential equations with variable coefficients. The proposed method is general and applicable to the free longitudinal vibration analysis of non-uniform rods with arbitrary shape, provided that the cross-sectional area function is differentiable. Unlike many existing approaches, the present formulation does not require problem-specific reformulation when the geometry changes, and it explicitly accounts for numerical stability through the choice of the approximation strategy. These features address important limitations of existing analytical and semi-analytical methods, which are often restricted to particular functional forms and sensitive to numerical conditioning.

Beyond theoretical interest, longitudinal vibration analysis of non-uniform rods is directly relevant to a range of practical engineering applications. In agricultural machinery, structural components such as shafts and supporting members often exhibit non-uniform cross-sections due to weight optimization and manufacturing constraints, where vibration characteristics significantly influence efficiency, durability, and operational quality [28]. Similarly, in special-purpose and military vehicles operating under demanding conditions, non-uniform structural elements are widely used to balance strength and weight requirements, and their vibration behavior plays a critical role in structural integrity and fatigue resistance [29]. These applications highlight the need for general and computationally efficient vibration analysis methods capable of handling arbitrary smoothly varying geometries without problem-specific reformulation.

MATERIALS AND METHODS

Differential transforms

Consider a rod of cross-sectional area $A(x)$ such that $A(x)$ and all of its all derivatives are continuous and smooth in the interval (x_0, x_1). The K^{th} derivative of $A(x)$ evaluated at a specific point x_v, is referred to as the $A(K)$ image of the original $A(x)$. The set of all images $A(K)$, for K= 0,1,2, ..., constitutes the differential spectrum of the function $A(x)$. The fundamental relation used to obtain the images from the original function is given as follows [10–12]:

$$A(K) = \frac{H^K}{K!} \frac{d^K A(x)}{dx^K}_{x=x_v}, \tag{1}$$

where: $A(K)$ denotes the differential transform image of $A(x)$; H is a predefined scaling parameter, and x_v is the center of approximation.

Once the set of images $A(K)$ is obtained, the original function can be reconstructed in several equivalent forms, depending on the chosen series representation. In particular, the inverse differential transform in the form of a differential Taylor series is expressed as

$$A(x) = \sum_{K=0}^{\infty} \left(\frac{x - x_v}{H}\right)^K A(K). \tag{2}$$

Table 1 summarizes the principal algebraic operations on functions in the x-domain and their corresponding images in the differential transform (DT) $K-$ domain [10–12]. Let us assume that the original functions $u(x)$ and $v(x)$ have differential spectra $U(K)$ and $V(K)$, respectively. The objective is then to determine $Z(K)$ which represents the differential spectrum of the function $z(x)$, based on the known spectra $U(K)$ and $V(K)$.

Table 1. Main algebraic operations in differential transformation domain

Original domain	DT domain
$z(x) = u(x) + v(x)$	$Z(K) = U(K) + V(K)$
$z(x) = cu(x)$	$Z(K) = cU(K)$
$z(x) = u(x)v(x)$	$Z(K) = \sum_{p=0}^{K} U(p)V(K-p)$
$z(x) = \frac{u(x)}{v(x)}$	$Z(K) = \frac{U(K) - \sum_{p=0}^{K} U(p)V(K-p)}{V(0)}$
$z(x) = \frac{du(x)}{dx}$	$Z(K) = (K+1)U(K+1)$
$z(x) = \frac{d^2u(x)}{dx^2}$	$Z(K) = (K+1)(K+2)U(K+2)$

As mentioned above, the proposed method is independent of the specific geometric shape of the rod. The only required condition is the successful evaluation of the differential spectrum $A(K)$ of the cross-sectional area function $A(x)$. The efficiency and generality of the proposed approach are demonstrated by solving a range of benchmark problems reported in the literature, including cases where $A(x) = (ax + b)^n$, $A(x) = \sin^2(ax + b)$, $A(x) = e^{cx^2}$. In addition, examples involving more complex cross-sectional variations are considered, such as $A(x) = e^{cx+1}[A_1\sin(ax + b) + A_2\cos(ax + b)]$. Such functional forms are generally not amenable to classical analytical solution techniques, which highlights the advantage of the proposed method.

There are two principal approaches for obtaining the differential spectrum $A(K)$ from the original function $A(x)$. The first approach relies on direct symbolic differentiation, whereby the K^{th}-order derivative of $A(x)$ is evaluated at the point x_v to obtain the corresponding image $A(K)$. Although straightforward, this approach becomes computationally inefficient for complicated functional forms of $A(x)$ and for relatively large values of K, due to the increasing complexity of higher-order derivatives. The second approach is based on the algebraic rules of differential transforms, which allow the differential spectrum of $A(x)$ to be constructed without explicit differentiation. For example, if $A(x) = e^{cx}\sin(ax + b)$, then its differential spectrum can be obtained directly using the operational properties of the differential transforms domain, as shown below.

$$A(K) = \sum_{p=0}^{K} \frac{a^p}{p!} \sin\left(ax_v + b + \frac{\pi p}{2}\right) \frac{c^{K-p}}{(K-p)!} e^{cx_v}.$$

Application of the differential transforms methods to non-uniform rod vibration

Consider a rod with a non-uniform cross-sectional area undergoing free longitudinal (axial) vibration, as shown in Figure 1, where $A(x)$ represents a function that describes the variation of the cross-sectional profile along the x axis. The classical assumptions of thin-rod electrodynamics are adopted, implying that the vibration problem is governed by a second-order partial differential equation in both time and space. By applying the separation of variables under synchronous harmonic motion, the governing equation is reduced to an ordinary differential equation containing the free vibration frequency parameter ω. The principal mathematical difficulty of this formulation arises from the presence of spatially varying coefficients, which precludes the direct application of standard solution techniques developed for uniform rods. From a mathematical standpoint, this problem can be classified as an eigenvalue problem for a linear differential operator with variable coefficients.

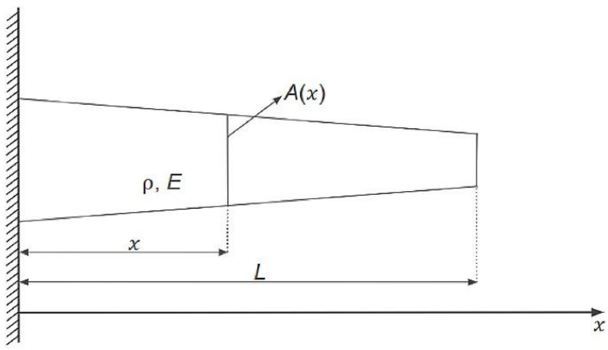

Figure 1. Parameters for analysis of free longitudinal vibration of a rod with variable cross-sectional area

The longitudinal motion of a rod with variable cross-section is governed by the following second-order ordinary differential equation [2]. The variable coefficient in the second term distinguishes this equation from its uniform counterpart:

$$\frac{d^2u}{dx^2}+\frac{1}{A(x)}\frac{dA(x)}{dx}\frac{du}{dx}+\frac{\rho}{E}\omega^2u=0, \tag{3}$$

where: $A(x)$ denotes the cross-sectional area as a function of the axial coordinate x, E is Young's modulus, and ρ is the mass density. The temporal dependence of the original partial differential equation is incorporated into the frequency-dependent term, assuming a harmonic solution in time. Introducing the notation $M(x)=\frac{1}{A(x)}\frac{dA(x)}{dx}$, the (3) can be rewritten in a form:

$$\frac{d^2u}{dx^2}+M(x)\frac{du}{dx}+\frac{\rho}{E}\omega^2u=0. \tag{4}$$

Here

$$M(x)=\frac{1}{A(x)}\frac{dA(x)}{dx}=\frac{dA(x)/dx}{A(x)}=\frac{D(x)}{A(x)},$$

where $D(x)$ is the first derivative of $A(x)$.

Since $D(x)$ is directly related to $A(x)$, its differential spectrum can be obtained from the differential spectrum of A(x) using the properties summarized in Table 1. Specifically, the differential spectrum of D(x) is given by $D(K)=(K+1)A(K+1)$. In the subsequent analysis, the scaling coefficient is taken as $\mathrm{H}=1$, without loss of generality. Using the differential transform rule for the division of two functions, the differential spectrum of $M(x)$ is obtained as:

$$M(K)=\frac{D(K)-\sum_{p=0}^{K-1}M(p)A(K-p)}{A(0)}=\frac{(K+1)A(K+1)-\sum_{p=0}^{K-1}M(p)A(K-p)}{A(0)}. \tag{5}$$

Alternatively, $M(x)$ may be expressed as the ratio of two functions,

$$M(x)=\frac{P(x)}{Q(x)}=\frac{dA(x)/dx}{A(x)},$$

which leads to the following general expression for its differential spectrum:

$$M(K)=\frac{P(K)-\sum_{p=0}^{K-1}M(p)Q(K-p)}{Q(0)}. \tag{6}$$

Both approaches yield identical results; however, depending on the functional form of $A(x)$, one approach may be computationally more efficient than the other. For instance, if $A(x)=(ax+b)^n$, then:

$$M(x)=\frac{na(ax+b)^{n-1}}{(ax+b)^n}=\frac{na}{(ax+b)}$$

and the corresponding differential spectrum is:

$$M(0)=\frac{na}{(ax_v+b)},$$
$$M(K)=-\frac{a}{(ax_v+b)}M(K-1)=(-1)^K n\frac{a^{K+1}}{(ax_v+b)^{K+1}}, K=1,2,\dots \tag{7}$$

If the center of approximation is chosen as $x_v = 0$ and $a > b$, the differential spectrum *M(K)* diverges, leading to numerical instability. For any other choice of $x_v \neq 0$, the series generally converges, since the denominator term $(ax_v)^{K+1}$prevents unbounded growth. From a computational standpoint, selecting $x_v = L/2$ for the interval *(*0*, L)* is often optimal, as it improves convergence and numerical stability. Applying the differential transform to (4) yields the following recurrence relation in the transform domain:

$$(K+1)(K+2)U(K+2) + \sum_{p=0}^{K} M(K-p)(p+1)U(p+1) + \frac{\rho}{E}\omega^2 U(K) = 0, \quad (8)$$

Rearranging leads to

$$U(K+2) = -\frac{1}{(K+1)(K+2)}\left[\sum_{p=0}^{K} M(K-p)(p+1)U(p+1) + \frac{\rho}{E}\omega^2 U(K)\right]. \quad (9)$$

By sequentially increasing K, the solution can be written in the recursive form

$$U(K+2) = B_K U(1) + C_K U(0), \quad (10)$$

where

$$\begin{gathered} B_K(\omega) = -\frac{1}{(K+1)(K+2)}\left[\sum_{p=1}^{K}(p+1)\, M(K-p)B_{p-1} + M(K) + \frac{\rho}{E}\omega^2 B_{K-2}\right], \\ C_K(\omega) = -\frac{1}{(K+1)(K+2)}\left[\sum_{p=1}^{K}(p+1)\, M(K-p)C_{p-1} + \frac{\rho}{E}\omega^2 C_{K-2}\right]. \end{gathered} \quad (11)$$

Since the initial values $U(0)$ and $U(1)$ are not known a priori, they are treated as independent variables, and the entire differential spectrum is expressed in terms of these quantities. The displacement field *u(x, ω)* and its derivative are then reconstructed using the inverse differential transform, as given by (12) and (13).

$$\begin{gathered} u(x,\omega) = U(0) + U(1)(x-x_v) + \cdots + U(K)(x-x_v)^K = \\ = U(0) + U(1)(x-x_v) + [B_0U(1) + C_0U(0)](x-x_v)^2 + \\ + \cdots + [B_{K-2}U(1) + C_{K-2}U(0)](x-x_v)^K = \\ = (1 + C_0(x-x_v)^2 + \cdots + C_{K-2}(x-x_v)^K)U(0) + \\ +\big((x-x_v) + B_0(x-x_v)^2 + \cdots + B_{K-2}(x-x_v)^K\big)U(1). \end{gathered} \quad (12)$$

The first derivative of $u(x,\omega)$ with respect to x is then given by

$$\begin{gathered} u'^{(x,\omega)} = U(1) + 2U(2)(x-x_v) + \cdots + KU(K)(x-x_v)^{K-1} \\ = U(1) + 2[B_0U(1) + C_0U(0)](x-x_v) + \cdots \\ +K[B_{K-2}U(1) + C_{K-2}U(0)](x-x_v)^{K-1} = (2C_0(x-x_v) + \cdots + KC_{K-2}(x-x_v)^{K-1})U(0) + \\ +(1 + 2B_0(x-x_v) + \cdots + KB_{K-2}(x-x_v)^{K-1})U(1). \end{gathered} \quad (13)$$

Equations 12 and 13 enable the direct imposition of boundary conditions in algebraic form. For a fixed–fixed rod, the boundary conditions are

$$u(0) = 0, u(L) = 0. \quad (14)$$

It will give us the following system of equations:

$$\begin{cases} (1 + C_0(-x_v)^2 + C_1(-x_v)^3 + \cdots + C_{K-2}(-x_v)^K)U(0) + \big((-x_v) + B_0(-x_v)^2 + B_1(-x_v)^3 + \cdots + B_{K-2}(-x_v)^K\big)U(1) = 0, \\ (1 + C_0(L-x_v)^2 + C_1(L-x_v)^3 + \cdots + C_{K-2}(L-x_v)^K)U(0) + \big((L-x_v) + B_0(L-x_v)^2 + \cdots + B_{K-2}(L-x_v)^K\big)U(1) = 0. \end{cases} \quad (15)$$

By notation

$$\begin{cases} f_{11} = & 1 + C_0(-x_v)^2 + C_1(-x_v)^3 + \cdots + C_{K-2}(-x_v)^K, \\ f_{12} = & (-x_v) + B_0(-x_v)^2 + B_1(-x_v)^3 + \cdots + B_{K-2}(-x_v)^K, \\ f_{21} = & 1 + C_0(L - x_v)^2 + C_1(L - x_v)^3 + \cdots + C_{K-2}(L - x_v)^K, \\ f_{22} = & (L - x_v) + B_0(L - x_v)^2 + B_1(L - x_v)^3 + \cdots + B_{K-2}(L - x_v)^K. \end{cases} \tag{16}$$

We will have

$$\begin{bmatrix} f_{11} & f_{12} \\ f_{21} & f_{22} \end{bmatrix} \begin{pmatrix} U(0) \\ U(1) \end{pmatrix} = 0. \tag{17}$$

As the $U(0) \neq 0$ and $U(1) \neq 0$, a nontrivial solution exists only if the determinant of the coefficient matrix vanishes, i.e.,

$$f_{11}f_{22} - f_{12}f_{21} = 0. \tag{18}$$

Equation 18 defines a characteristic polynomial in ω; its roots correspond to the natural frequencies of the rod. For the fixed-free rod, the boundary conditions are:

$$u(0) = 0, u'(L) = 0 \tag{19}$$

The corresponding system of equations will be

$$\begin{Bmatrix} (1 + C_0(-x_v)^2 + C_1(-x_v)^3 + \cdots + C_{K-2}(-x_v)^K)U(0) + \left((-x_v) + B_0(-x_v)^2 + B_1(-x_v)^3 + \cdots + B_{K-2}(-x_v)^K\right)U(1) = 0, \\ (2C_0(L - x_v) + 3C_1(L - x_v)^2 + \cdots + KC_{K-2}(L - x_v)^{K-1})U(0) + +(1 + 2B_0(L - x_v) + \cdots + KB_{K-2}(L - x_v)^{K-1})U(1) = 0. \end{Bmatrix} \tag{20}$$

Defining

$$\begin{cases} f_{11} = & 1 + C_0(-x_v)^2 + C_1(-x_v)^3 + \cdots + C_{K-2}(-x_v)^K, \\ f_{12} = & (-x_v) + B_0(-x_v)^2 + B_1(-x_v)^3 + \cdots + B_{K-2}(-x_v)^K, \\ f_{21} = & 2C_0(L - x_v) + 3C_1(L - x_v)^2 + \cdots + KC_{K-2}(L - x_v)^{K-1}, \\ f_{22} = & 1 + 2B_0(L - x_v) + 2B_1(L - x_v)^2 + \cdots + KB_{K-2}(L - x_v)^{K-1}, \end{cases} \tag{21}$$

the characteristic equation is again

$$f_{11}f_{22} - f_{12}f_{21} = 0,$$

whose roots yield the natural frequencies.

For free-free case the boundary conditions are:

$$u'^{(0)} = 0, u'(L) = 0. \tag{22}$$

The corresponding system of equations will be

$$\begin{Bmatrix} (2C_0(-x_v) + 3C_1(-x_v)^2 + \cdots + KC_{K-2}(-x_v)^{K-1})U(0) + (1 + 2B_0(-x_v) + 2B_1(-x_v)^2 + \cdots + KB_{K-2}(-x_v)^{K-1})U(1) = 0, \\ (2C_0(L - x_v) + 3C_1(L - x_v)^2 + \cdots + KC_{K-2}(L - x_v)^{K-1})U(0) + (1 + 2B_0(L - x_v) + \cdots + KB_{K-2}(L - x_v)^{K-1})U(1) = 0. \end{Bmatrix} \tag{23}$$

By notation

$$\begin{cases} f_{11} = & 2C_0(-x_v) + 3C_1(-x_v)^2 + \cdots + KC_{K-2}(-x_v)^{K-1}, \\ f_{12} = & 1 + 2B_0(-x_v) + 3B_1(-x_v)^2 + \cdots + KB_{K-2}(-x_v)^{K-1}, \\ f_{21} = & 2C_0(L - x_v) + 3C_1(L - x_v)^2 + \cdots + KC_{K-2}(L - x_v)^{K-1}, \\ f_{22} = & 1 + 2B_0(L - x_v) + 3B_1(L - x_v)^2 + \cdots + KB_{K-2}(L - x_v)^{K-1}, \end{cases} \tag{24}$$

the characteristic equation remains

$$f_{11}f_{22} - f_{12}f_{21} = 0.$$

In summary, for any prescribed boundary conditions, the proposed DTM formulation reduces the original variable-coefficient eigenvalue problem to a finite-dimensional algebraic system, whose characteristic polynomial is obtained explicitly and whose roots directly yield the natural frequencies of the non-uniform rod.

For clarity and ease of implementation, the complete computational procedure of the proposed DTM can be summarized in the following steps (Figure 2). Flowchart illustrates the unified computational procedure of the proposed DTM for free longitudinal vibration analysis of non-uniform rods with arbitrary differentiable cross-sectional area functions. The workflow highlights the geometry-invariant nature of the formulation, in which only the differential spectrum of the cross-sectional area function is required, while the overall solution procedure remains unchanged.

It should be emphasized that the independence of the proposed method from the specific geometric shape of the rod is understood in a computational sense. The formulation remains unchanged for any cross-sectional area function $A(x)$ that is sufficiently smooth (differentiable) over the domain, as only its differential spectrum $A(K)$ is required. Consequently, the approach is directly applicable to a broad class of non-uniform rods with smoothly varying geometries. However, rods with sharp geometric discontinuities, such as stepped or piecewise-constant cross-sections, lie outside the direct scope of the present formulation and would require a modified or piecewise implementation of the differential transform procedure.

From a theoretical standpoint, the main contribution of this work lies in the development of a unified eigenvalue formulation for longitudinal vibration problems of non-uniform rods governed by variable-coefficient differential equations. Unlike many existing analytical and semi-analytical approaches, which are typically derived for specific cross-sectional profiles and require separate formulations for different boundary conditions, the proposed DTM accommodates fixed–fixed, fixed–free, and free–free boundary conditions within a single recursive algebraic structure. The governing equations, recursion relations, and displacement reconstruction procedure remain invariant, while the effect of boundary conditions is introduced exclusively through the resulting characteristic polynomial. This clear separation between geometric variability and boundary-condition enforcement provides a transparent and systematic theoretical framework for modal analysis of non-uniform rods and constitutes a meaningful extension of differential-transform-based vibration theory.

RESULTS AND DISCUSSION

Here, we consider various examples from the literature to assess the generality and accuracy of the proposed method. It is important to note that literature does not provide a single unified approach applicable to arbitrary cross-sectional area functions. Instead, for each particular form of $A(x)$, specialized techniques have been developed, which are typically not transferable to other types of $A(x)$. Accordingly, benchmarking against representative published cases is essential.

We begin with the examples reported in [30], where the cross-sectional area varies as $A(x) = 2-x$ and $A(x)=3-4x+2x^2$. Table 2 lists the corresponding non-dimensional natural frequencies for fixed–free rods. The obtained results are essentially identical to those reported by Eisenberger [30].

Next, we consider the case studied by Abrate [1], where the cross-sectional area is given by $A(x)=(ax+b)^2$. Tables 3 and 4 present the

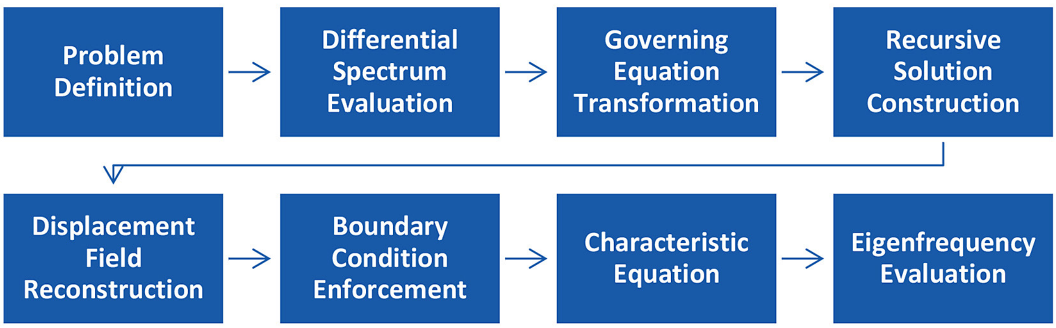

Figure 2. Flowchart of the proposed computational procedure

Table 2. Non-dimensional natural frequencies of fixed-free rods

Mode	$A(x)$ = 2 – x		$A(x)$ = 3 – 4x + 2x^2	
	Proposed	Eisenberger [30]	Proposed	Eisenberger [30]
1	1.794010905	1.79401	1.97089606	1.9709
2	4.802060761	4.80206	4.820757255	4.82076
3	7.908961712	7.90896	7.918202749	7.9182
4	11.03509458	11.03509	11.04144264	11.04144
5	14.16798651	14.16799	14.17284442	14.17284

Table 3. Non-dimensional natural frequencies of fixed-free rods with $A(x)=(ax+b)^2$

Mode	a = 1, b = 1			a = 2, b = 1		
	Proposed	Rayleigh-Ritz	Abrate [1]	Proposed	Rayleigh-Ritz	Abrate [1]
1	1.165561	1.165615	1.165561	0.967403	0.967665	0.967403
2	4.604217	4.604376	4.604217	4.567452	4.568147	4.567452
3	7.789884	7.790158	7.789884	7.768373	7.769588	7.768373
4	10.949944	10.950418	10.949944	10.934682	10.936704	10.934682
5	14.101725	14.102380	14.101725	14.089887	14.092781	14.089887
6	17.249782	17.251001	17.249782	17.240109	17.245095	17.240109

Table 4. Non-dimensional natural frequencies of free-free rods with $A(x)=(ax+b)^2$

Mode	a = 1, b = 1			a = 2, b = 1		
	Proposed	Rayleigh-Ritz	Abrate [1]	Proposed	Rayleigh-Ritz	Abrate [1]
1	3.286007	3.286008	3.286007	3.474336	3.474340	3.474335
2	6.360678	6.360685	6.360678	6.480031	6.480061	6.480031
3	9.477196	9.477235	9.477196	9.561368	9.561516	9.561368
4	12.605890	12.605965	12.605891	12.670360	12.670688	12.670360
5	15.739656	15.739950	15.739650	15.791750	15.792848	15.792159
6	18.876001	18.876462	18.875239	18.919653	18.921643	18.918810

non-dimensional natural frequencies for fixed–free and free–free rods, respectively.

The results show excellent agreement with those reported in [1] and with the Rayleigh–Ritz approximation [31]. In the Rayleigh–Ritz computations, 10 admissible functions were used, and the required symbolic integrations were carried out in MATLAB.

We next examine the example from [2], where the cross-sectional area varies according to $A(x)=\sin^2(ax+b)$. Tables 5 and 6 report the non-dimensional natural frequencies for fixed–fixed and fixed–free rods, respectively. The obtained results are in very good agreement with the values reported in [2]. Figures 3 and 4 illustrate the convergence behavior of the natural frequencies with respect to the truncation order K for case $a = 2$.

Table 7 summarizes the results for free–free rods. In this case, the proposed results differ from those reported in [2]; however, a correction was later published in [32], and the authors acknowledged the correction in [33]. The present results are in close agreement with the corrected values reported in [32]. Figure 5 shows the convergence of the free–free natural frequencies with respect to K.

We also consider another benchmark example from [2], where the cross-sectional area varies according to $A(x) = (ax + b)^2$. The non-dimensional natural frequencies obtained using the proposed method are compared with the values reported in [2], as well as with independent results obtained using the Rayleigh–Ritz method and the finite element method (FEM) [5-7], as summarized in Tables 8–10. As shown in these tables, the results produced by the proposed DTM are in excellent agreement with both the Rayleigh–Ritz and FEM solutions for all considered boundary conditions and parameter

Table 5. Non-dimensional natural frequencies of fixed-fixed rods with $A(x)=\sin^2(ax+b)$

Mode	a = 1, b = 1		a = 2, b = 1	
	Proposed	Kumar [2]	Proposed	Kumar [2]
1	2.978188	2.978189	2.422727	2.422727
2	6.203097	6.203097	5.956377	5.956376
3	9.371576	9.371576	9.210128	9.210127
4	12.526519	12.526719	12.406197	12.406195
5	15.676100	15.676100	15.580120	15.580119
6	18.823011	18.823011	18.743154	18.743152

Table 6. Non-dimensional natural frequencies of fixed-free rods with $A(x)=\sin^2(ax+b)$

Mode	a = 1, b = 1		a = 2, b = 1	
	Proposed	Kumar [2]	Proposed	Kumar [2]
1	1.517637	1.517638	2.148560	2.148560
2	4.702145	4.702145	5.535763	5.535762
3	7.848311	7.848311	8.632812	8.632812
4	10.991621	10.991620	11.694643	11.694640
5	14.134123	14.134120	14.757861	14.757860
6	17.276282	17.276280	17.830601	17.830600

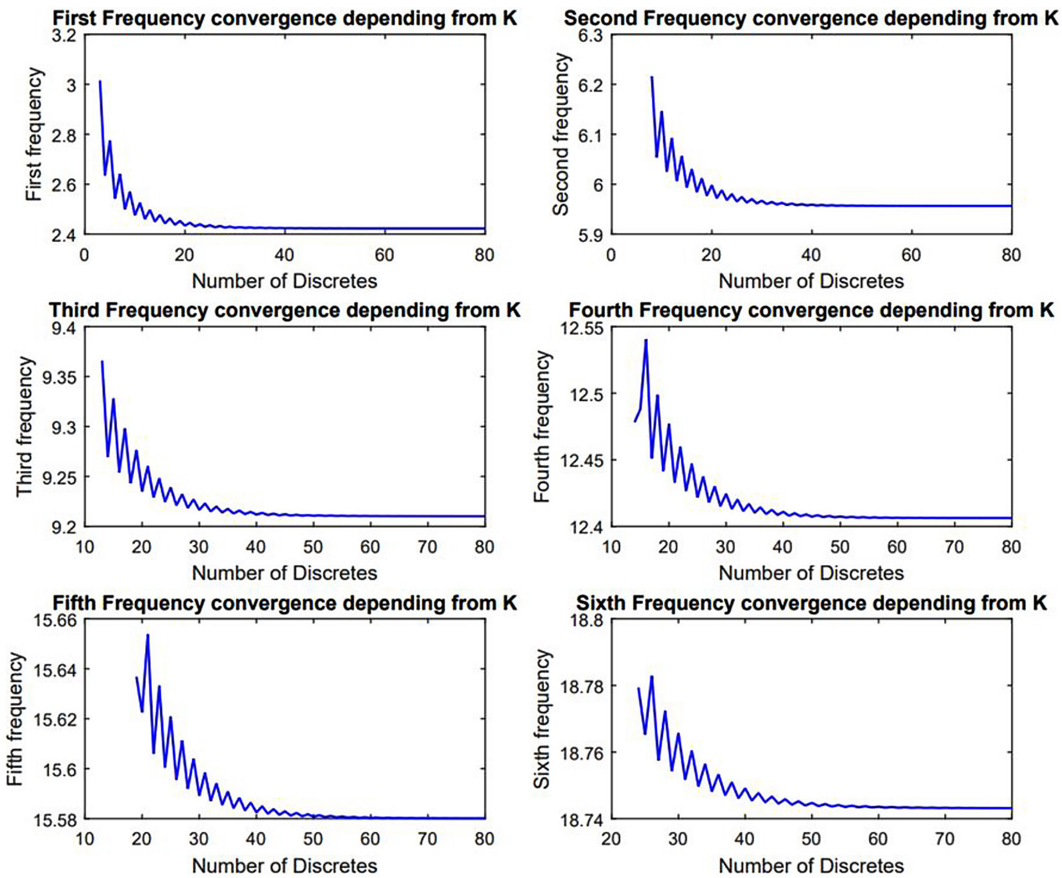

Figure 3. Natural frequencies convergence for fixed-fixed rod

values. In particular, the FEM results obtained using a MATLAB implementation coincide with the Rayleigh–Ritz values up to at least five significant digits, thereby providing strong independent numerical validation of the present formulation. This three-way agreement (proposed method–Rayleigh–Ritz–FEM)

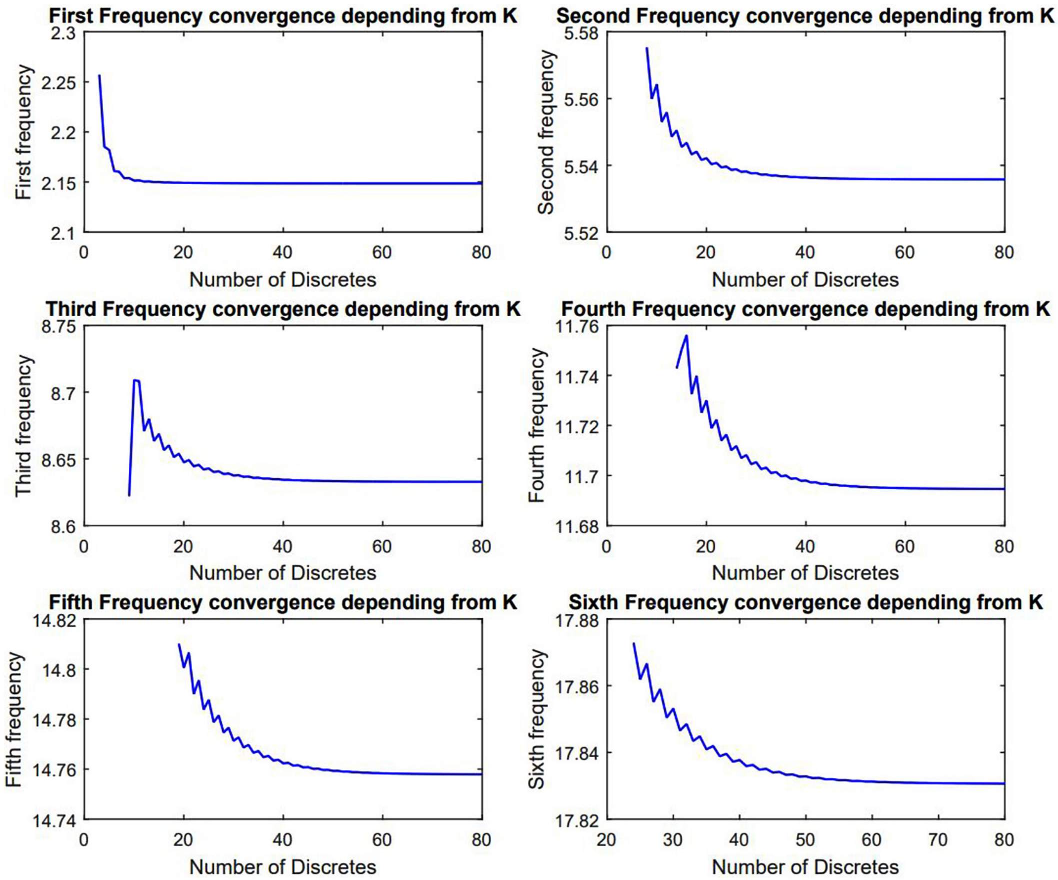

Figure 4. Natural frequencies convergence for fixed-free rod

Table 7. Non-dimensional natural frequencies of free-free rods with $A(x)=\sin^2(ax+b)$

Mode	*a* = 1		*a* = 2	
	Proposed	Kumar [2] / Yardimoglu [32]	Proposed	Kumar [2] / Yardimoglu [32]
1	3.309070	3.0004297	4.209605	1.5808147
		3.309070		4.209604
2	6.375208	6.216901	7.259860	5.113309
		6.375209		7.259860
3	9.487363	9.380888	10.283501	8.436760
		9.487363		10.283498
4	12.613648	12.533530	13.317981	11.721540
		12.613648		13.317980
5	15.745913	15.681720	16.368924	14.977670
		15.745913		16.368917
6	18.881240	18.827700	19.435338	18.210650
		18.881240		19.435335

clearly confirms the accuracy and robustness of the present results for this challenging case. In contrast, noticeable discrepancies are observed when comparing the present results with those reported in [2]. These deviations are systematic across all boundary conditions and become especially pronounced for the fixed–free configuration. The FEM results confirm the existence of a well-defined fundamental longitudinal mode for all tested values of the parameter *a*, in full agreement with the proposed method

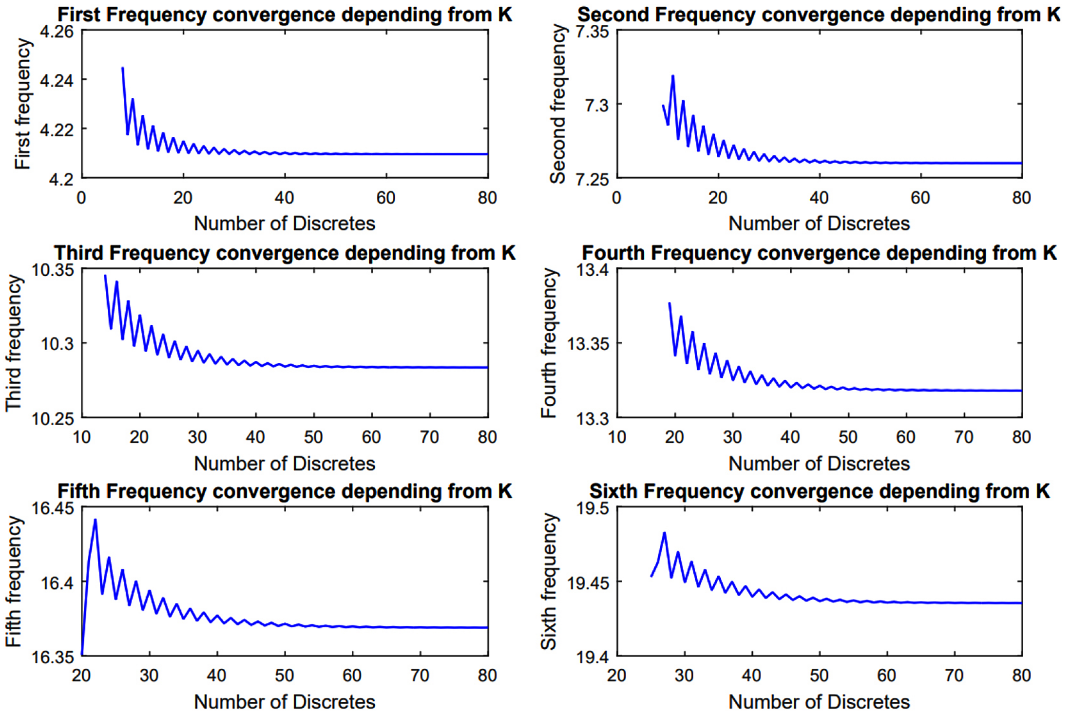

Figure 5. Natural frequencies convergence for free-free rod

and the Rayleigh–Ritz approximation. This finding directly contradicts the claim made in [2] that the first mode disappears for $a > 0.97$, a behavior that is physically implausible for a well-posed longitudinal vibration problem.

The observed inconsistencies in [2] are therefore most plausibly attributed to inaccuracies in the solution of the transcendental characteristic equation used therein to determine the eigenfrequencies, rather than to any physical effect or limitation of the present formulation. It is worth noting that the proposed method successfully reproduces the results of the literature for all other benchmark cases considered in this study, including those reported in [3, 4], further supporting the reliability of the present results for the $(ax+b)^4$ cross-sectional profile.

Overall, the excellent agreement between the proposed method, the Rayleigh–Ritz approximation (using 18 trial functions), and the FEM benchmark demonstrates that the present DTM provides accurate, stable, and physically consistent predictions for free longitudinal vibrations of non-uniform rods, even in cases where earlier analytical treatments exhibit numerical or formulation-related deficiencies.

We now consider the example from [3], where the cross-sectional area varies as $A(x)=x^n e^{bx^2}$. In this case, the axial coordinate spans the interval $L_1 < x < L_2$, and the boundary conditions are:

$$\text{Fixed – Fixed rod}: u(L_1, t) = u(L_2, t) = 0,$$
$$\text{Fixed – Free rod}: u(L_1, t) = u'(L_2, t) = 0,$$
$$\text{Free – Free rod}: u'(L_1, t) = u'(L_2, t) = 0. \quad (25)$$

The corresponding boundary conditions in the DT domain are given by (26)–(28).

- For fixed-fixed rod:

$$\begin{cases} \left(1 + C_0(L_1 - x_v)^2 + \cdots + C_{K-2}(L_1 - x_v)^K\right)U(0) + \left((L_1 - x_v) + B_0(L_1 - x_v)^2 + \cdots + B_{K-2}(L_1 - x_v)^K\right)U(1) = 0 \\ \left(1 + C_0(L_2 - x_v)^2 + \cdots + C_{K-2}(L_2 - x_v)^K\right)U(0) + \left((L_2 - x_v) + B_0(L_2 - x_v)^2 + \cdots + B_{K-2}(L_2 - x_v)^K\right)U(1) = 0 \end{cases} \quad (26)$$

- For fixed-free rod:

$$\begin{cases} \left(1 + C_0(L_1 - x_v)^2 + C_1(L_1 - x_v)^3 + \cdots + C_{K-2}(L_1 - x_v)^K\right)U(0) + \left((L_1 - x_v) + B_0(L_1 - x_v)^2 + \cdots + B_{K-2}(L_1 - x_v)^K\right)U(1) = 0 \\ \left(2C_0(L_2 - x_v) + 3C_1(L_2 - x_v)^2 + \cdots + KC_{K-2}(L_2 - x_v)^{K-1}\right)U(0) + \left(1 + 2B_0(L_2 - x_v) + \cdots + KB_{K-2}(L_2 - x_v)^{K-1}\right)U(1) = 0 \end{cases} \quad (27)$$

- For free-free rod:

$$\begin{cases} \left(2C_0(L_1 - x_v) + 3C_1(L_1 - x_v)^2 + \cdots + KC_{K-2}(L_1 - x_v)^{K-1}\right)U(0) + \left(1 + 2B_0(L_1 - x_v) + \cdots + KB_{K-2}(L_1 - x_v)^{K-1}\right)U(1) = 0 \\ \left(2C_0(L_2 - x_v) + 3C_1(L_2 - x_v)^2 + \cdots + KC_{K-2}(L_2 - x_v)^{K-1}\right)U(0) + \left(1 + 2B_0(L_2 - x_v) + \cdots + KB_{K-2}(L_2 - x_v)^{K-1}\right)U(1) = 0 \end{cases} \quad (28)$$

Table 8. Non-dimensional natural frequencies of fixed-fixed rods with $A(x)=(ax+b)^4$

Mode	*a* = 1, *b* = 1				*a* = 2, *b* = 1			
	Proposed	Rayleigh-Ritz	Kumar	FEM	Proposed	Rayleigh-Ritz	Kumar	FEM
1	3.286007	3.286076	3.133487	3.286008	3.474336	3.474590	2.386221	3.474338
2	6.360678	6.360846	6.278921	6.360686	6.480031	6.480687	6.272251	6.480039
3	9.477196	9.477429	9.421905	9.477221	9.561368	9.562345	9.417264	9.561394
4	12.605890	12.606256	12.564210	12.605948	12.670360	12.671858	12.560670	12.670421
5	15.739656	15.740083	15.706230	15.739769	15.791750	15.793589	15.703370	15.791866
6	18.876001	18.876626	18.848110	18.876197	18.919653	18.922240	18.845270	18.919852

Table 9. Non-dimensional natural frequencies of fixed-free rods with $A(x)=(ax+b)^4$

Mode	*a* = 1, *b* = 1				*a* = 2, *b* = 1			
	Proposed	Rayleigh-Ritz	Kumar [2]	FEM	Proposed	Rayleigh-Ritz	Kumar [2]	FEM
1	0.824971	0.825011	-	0.824972	0.526694	0.526886	-	0.526695
2	4.600454	4.600562	4.487482	4.600458	4.689329	4.689777	4.404069	4.689334
3	7.789097	7.789283	7.721747	7.789112	7.848695	7.849530	7.672932	7.848711
4	10.949659	10.949938	10.901630	10.949699	10.993611	10.994879	10.866970	10.993652
5	14.101592	14.101960	14.064260	14.101675	14.136235	14.137945	14.037360	14.136321
6	17.249709	17.250211	17.219170	17.249860	17.278247	17.280554	17.197190	17.278402

Table 10. Non-dimensional natural frequencies of free-free rods with $A(x)=(ax+b)^4$

Mode	*a* = 1, *b* = 1				*a* = 2, *b* = 1			
	Proposed	Rayleigh-Ritz	Kumar [2]	FEM	Proposed	Rayleigh-Ritz	Kumar [2]	FEM
1	3.555788	3.555788	3.378458	3.555789	4.041322	4.041323	3.286891	4.041324
2	6.513068	6.513070	6.425906	6.513076	6.857174	6.857180	6.614998	6.857182
3	9.581270	9.581277	9.524152	9.581295	9.829987	9.830014	9.671519	9.830013
4	12.684608	12.684622	12.642120	12.684667	12.876552	12.876613	12.759890	12.876612
5	15.802877	15.802911	15.769030	15.802991	15.958453	15.958601	15.866250	15.958569
6	18.928798	18.928850	18.900660	18.928993	19.059360	19.059607	18.983120	19.059557

Table 11. Fundamental frequency for fixed-fixed rods with $A(x)=x^n e^{bx^2}$

Parameter	n	b							
		-3	-2	-1	-0.5	0.5	1	2	3
Raj [3]	-2	4.885	4.546	4.280	4.180	4.058	4.038	4.082	4.226
Proposed		4.8850	4.5455	4.2787	4.1791	4.0577	4.0382	4.0819	4.2265
Raj [3]	0	3.206	3.068	3.043	3.077	3.235	3.356	3.663	4.015
Proposed		3.2058	3.0684	3.0431	3.0770	3.2354	3.3557	3.6626	4.0345
Raj [3]	1	2.479	2.518	2.686	2.816	3.152	3.349	3.787	4.260
Proposed		2.4792	2.5176	2.6864	2.8163	3.1515	3.3491	3.7866	4.2599
Raj [3]	2	2.068	2.327	2.695	2.910	3.386	3.642	4.173	4.720
Proposed		2.0681	2.3270	2.6946	2.9099	3.3864	3.6415	4.1731	4.7199
Raj [3]	3	2.094	2.525	3.023	3.290	3.850	4.140	4.731	5.328
Proposed		2.0941	2.5254	3.0227	3.2898	3.8500	4.1397	4.7305	5.3278

These conditions represent a more general formulation than (15), (20), and (23), which can be recovered as special cases. Tables 11 and 12 list the fundamental and first overtone frequencies for fixed–fixed rods. The results are very close to those reported in [3]. The authors note that the proposed method can be used only for cases when the n is an integer. However, as there is a variant

Table 12. First overtone for fixed-fixed rods with $A(x)=x^n e^{bx^2}$

Parameter	n	b							
		-3	-2	-1	-0.5	0.5	1	2	3
Raj [3]	-2	7.580	7.367	7.209	7.151	7.081	7.069	7.090	7.173
Proposed		7.5798	7.3668	7.2089	7.1514	7.0812	7.0688	7.0902	7.1731
Raj [3]	0	6.355	6.262	6.238	6.252	6.331	6.397	6.573	6.811
Proposed		6.3552	6.2616	6.2378	6.2519	6.3314	6.3961	6.5733	6.8109
Raj [3]	1	5.992	5.976	6.034	6.090	6.252	6.357	6.612	6.921
Proposed		5.9919	5.9763	6.0344	6.0902	6.2522	6.3572	6.6119	6.9212
Raj [3]	2	5.864	5.934	6.075	6.171	6.404	6.552	6.871	7.238
Proposed		5.8642	5.9336	6.0753	6.1714	6.4098	6.5505	6.8708	7.2380
Raj [3]	3	5.976	6.126	6.344	6.475	6.773	6.936	7.317	7.727
Proposed		5.9761	6.1272	6.3442	6.4750	6.7769	6.9461	7.3173	7.7275

Table 13. Fundamental frequency for fixed-free rods with $A(x)=x^n e^{bx^2}$

Parameter	n	b							
		-3	-2	-1	-0.5	0.5	1	2	3
Raj [3]	-2	4.494	3.946	3.399	3.129	2.603	2.350	1.874	1.447
Proposed		3.7521	3.3661	2.9556	2.7440	2.3171	2.1056	1.6973	1.3220
Raj [3]	0	2.791	2.377	1.9966	1.765	1.384	1.207	0.891	0.630
Proposed		2.5315	2.1815	1.8239	1.6462	1.3029	1.1416	0.8488	0.6050
Raj [3]	1	1.924	1.594	1.274	1.121	0.840	0.715	0.501	0.338
Proposed		1.8229	1.5208	1.2229	1.0798	0.8142	0.6950	0.4897	0.3311
Raj [3]	2	1.169	0.931	0.710	0.610	0.435	0.359	0.241	0.156
Proposed		1.1410	0.9118	0.6981	0.6004	0.4289	0.3565	0.2389	0.1546
Raj [3]	3	0.617	0.468	0.341	0.285	0.194	0.158	0.101	0.064
Proposed		0.6115	0.4651	0.3382	0.2836	0.1932	0.1571	0.1014	0.0635

Table 14. Fundamental frequency for free-free rods with $A(x)=x^n e^{bx^2}$

Parameter	n	b							
		-3	-2	-1	-0.5	0.5	1	2	3
Raj [3]	-2	4.720	4.173	3.642	3.386	2.910	2.695	2.327	2.068
Proposed		4.7199	4.1731	3.6415	3.3864	2.9099	2.6946	2.3270	2.0681
Raj [3]	0	4.034	3.663	3.356	3.235	3.077	3.043	3.068	3.206
Proposed		4.0345	3.6626	3.3557	3.2354	3.0770	3.0431	3.0684	3.2058
Raj [3]	1	4.048	3.792	3.624	3.581	3.581	3.624	3.792	4.048
Proposed		4.0479	3.7918	3.6245	3.5809	3.5809	3.6245	3.7918	4.0479
Raj [3]	2	4.226	4.082	4.038	4.047	4.179	4.279	4.546	4.885
Proposed		4.2265	4.0819	4.0382	4.0577	4.1791	4.2787	4.5455	4.8850
Raj [3]	3	4.495	4.450	4.509	4.578	4.792	4.933	5.273	5.675
Proposed		4.4949	4.4500	4.5091	4.5783	4.7917	4.9327	5.2728	5.6748

of fractional differential transformations [34], so maybe it also could be applied for non-integer n.

Tables 13 and 14 present the fundamental frequencies for fixed–free and free–free boundary conditions. For the fixed–free case, some noticeable deviations from [3] occur, particularly for $n = -2$, 0, and 1. In contrast, for the free–free case, the results are almost identical to those in [3]. This pattern suggests that the fixed–free configuration may be more sensitive to the implementation details of boundary conditions and truncation order, and it warrants additional verification.

Table 15. Non-dimensional natural frequencies of fixed-fixed rods with $A(x) = e^{0.5x^2}$

Mode	Proposed	Kummer [4]	WKB [4]	Guo [4]
1	3.231130281	3.231130281	3.231128547	3.231130556
2	6.329186675	6.329186675	6.329186672	6.329186675
3	9.455600357	9.455600357	9.455600357	9.455600357
4	12.589528186	12.58952819	12.58952819	12.58952819

Table 16. Non-dimensional natural frequencies of fixed-fixed rods with $A(x) = e^{x^2}$

Mode	Proposed	Kummer [4]	WKB [4]	Guo [4]
1	3.339335867	3.339335867	3.339290046	3.339359214
2	6.387440254	6.387440254	6.387492001	6.387440261
3	9.494964058	9.494964058	9.494964055	9.494964058
4	12.619190216	12.61919022	12.61919022	12.61919022

Table 17. Non-dimensional natural frequencies of fixed-fixed rods with $A(x) = e^{2x^2}$

Mode	Proposed	Kummer [4]	WKB [4]	Guo [4]
1	3.603139793	3.603139793	3.602727427	3.607785468
2	6.539562675	6.539562675	6.539566227	6.539562927
3	9.598980427	9.598980427	9.598980578	9.598980426
4	12.697886705	12.69788671	12.69788672	12.69788670

Next, we consider the example where $A(x) = e^{cx^2/L}$. Tables 15–17 report the non-dimensional natural frequencies for L = 1. The obtained frequencies are consistent with the trends and observations reported in [4] and demonstrate excellent agreement across the compared methods.

Finally, to demonstrate the computational capability of the proposed approach, we consider a more complex cross-sectional variation of the form $A(x) = e^{cx+1}(\sin(ax+1) + \cos(ax+1))$. This functional form is not readily amenable to the classical techniques used in the above-cited studies, which are typically tailored to specific classes of $A(x)$. The computed non-dimensional natural frequencies for various parameter combinations are reported in Tables 18–20.

Overall, the results demonstrate that the proposed DTM formulation provides a unified computational procedure that remains unchanged for arbitrary differentiable cross-sectional area functions $A(x)$, thereby avoiding case-specific reformulations commonly required by classical approaches. In addition, the numerical stability and convergence of the method are strongly influenced by the choice of the approximation center x_v; selecting x_v within the analysis interval (e.g., $x_v = L/2$) significantly improves conditioning of the differential spectra and ensures robust evaluation of the characteristic polynomial roots. These features collectively highlight the generality, practicality, and reliability of the proposed framework for non-uniform rod vibration problems.

Despite the apparent simplicity of the governing equation, the numerical examples considered in this study involve a wide range of increasing complexity, including high-order polynomial, exponential, trigonometric, and composite cross-sectional functions. In particular, cases such as $A(x) = (ax + b)^4$ and $A(x) = e^{cx+1}(\sin(ax+1) + \cos(ax+1))$ lead to strongly variable coefficients and high-degree characteristic polynomials, which represent challenging benchmarks for eigenvalue-based vibration analysis. The results demonstrate that the proposed method remains stable and accurate even under such conditions, provided that the truncation order and approximation center are chosen appropriately.

The main limitations of the present formulation arise from its underlying assumptions: linear elastic material behavior, small-amplitude longitudinal vibrations, and differentiable cross-sectional profiles. Problems involving geometric discontinuities, material nonlinearity, damping, or pre-stress effects would require extensions of

Table 18. Non-dimensional natural frequencies of fixed-fixed rods with $A(x) = e^{cx+1}(\sin(ax+1) + \cos(ax+1))$

Mode	c=1	c=2	c=0.5	c=-2	c=1
	a=1	a=1	a=1	a=1	a=0.5
1	2.98466522	3.03167739	2.99224347	3.32373501	3.13864774
2	6.19784012	6.21830200	6.20272966	6.37601594	6.28148811
3	9.36636735	9.37942203	9.36985111	9.48666392	9.42361586
4	12.52206926	12.53167941	12.52475249	12.61274634	12.56549081
5	15.67231884	15.67993452	15.67449387	15.74504063	15.70725635
6	18.81975440	18.82606651	18.82158045	18.88044064	18.84896542

Table 19. Non-dimensional natural frequencies of fixed-free rods with $A(x) = e^{cx+1}(\sin(ax+1) + \cos(ax+1))$

Mode	c=1	c=2	c=0.5	c=-2	c=1
	a=1	a=1	a=1	a=1	a=0.5
1	1.55011739	1.25091748	1.71131780	2.61193545	1.34204360
2	4.75091752	4.67228750	4.80866274	5.25526869	4.64879666
3	7.88367957	7.83570925	7.91926032	8.20627706	7.81626796
4	11.01854930	10.98405064	11.04419724	11.25378345	10.96872106
5	14.15568062	14.12876303	14.17571017	14.34029271	14.11630818
6	17.29419322	17.27213229	17.31061597	17.44594668	17.26170451

Table 20. Non-dimensional natural frequencies of free-free rods with $A(x) = e^{cx+1}(\sin(ax+1) + \cos(ax+1))$

Mode	c=1	c=2	c=0.5	c=-2	c=1
	a=1	a=1	a=1	a=1	a=0.5
1	3.29980371	3.34365268	3.30602404	3.60593512	3.18881587
2	6.37866994	6.39848255	6.38345460	6.55210728	6.30713038
3	9.49194975	9.50476259	9.49542194	9.61087682	9.44078560
4	12.61787465	12.62737063	12.62055813	12.70799069	12.57838817
5	15.74962463	15.75717813	15.75180140	15.82206522	15.71758172
6	18.88449239	18.89076713	18.88632001	18.94501822	18.85757329

Table 21. Comparative summary

Aspect	Differential transform method (DTM)	FEM (1D axial)	Rayleigh–Ritz
Reformulation for new A(x)	Not required (only A(K))	Not required	Required
Matrix size	Small (K×K recursion)	Large (Ne×Ne)	Moderate
Typical DOFs (degrees of freedom)	K ≈ 40–80	N_e ≈ 200–1200	10–20 trial functions
Convergence control	Via truncation order K	Via mesh refinement	Via basis size
High-mode sensitivity	Moderate	High (mesh-dependent)	Moderate
Computational cost	Very low	High	Moderate
Mode shapes	Reconstructed analytically	Directly available	Available
Discontinuous (A(x))	Requires modification	Naturally handled	Difficult

the current framework and are therefore identified as directions for future research.

The comparative summary presented in Table 21 highlights the relative strengths and limitations of the DTM in relation to the finite element method (FEM) and the Rayleigh–Ritz approach. A key advantage of the proposed method is that it does not require reformulation when the cross-sectional area function $A(x)$ is changed; only the corresponding differential spectrum $A(K)$ must be updated. This contrasts with the Rayleigh–Ritz method, where the trial functions and formulation often need to be adapted to each specific geometry. From a computational standpoint, the DTM operates with a small recursive system controlled by the count of discrets K, typically requiring far fewer degrees of freedom than FEM discretizations. As a result, the computational cost of the proposed method is significantly lower, while still delivering accurate results for the low and moderate vibration modes that are of primary engineering interest. FEM, although highly versatile and capable of handling discontinuous cross-sectional profiles, generally requires a large number of elements to achieve comparable accuracy and exhibits increased sensitivity to mesh refinement, particularly for higher modes. The Rayleigh–Ritz method provides a useful semi-analytical alternative with moderate computational effort; however, its accuracy and convergence strongly depend on the choice and number of admissible trial functions. In contrast, the convergence behavior of the proposed DTM is directly controlled through the truncation order, offering a transparent and systematic means of balancing accuracy and efficiency.

It should be noted that the present formulation of the DTM assumes a differentiable cross-sectional area function, which represents its main limitation when compared to FEM. Problems involving sharp geometric discontinuities, such as stepped rods, would require either a modified formulation or a piecewise treatment. Nevertheless, for a broad class of smoothly varying geometries, the proposed method offers an effective compromise between generality, numerical stability, and computational efficiency.

Overall, this comparison demonstrates that the proposed DTM complements existing numerical and semi-analytical techniques by providing a unified, low-cost, and robust framework for the longitudinal vibration analysis of non-uniform rods, particularly well-suited to parametric studies and problems involving arbitrary differentiable cross-sectional profiles.

CONCLUSIONS

This study developed a unified and computationally efficient differential transforms method for the free longitudinal vibration analysis of non-uniform rods with arbitrarily varying, differentiable cross-sectional area functions. The original variable-coefficient eigenvalue problem was systematically reduced to a recursive algebraic formulation, leading to a characteristic polynomial whose roots determine the natural frequencies. A key outcome of the proposed approach is that the computational procedure remains invariant with respect to the functional form of the cross-sectional area, requiring only its differential spectrum and eliminating the need for case-specific reformulation.

The obtained numerical results demonstrate high accuracy and robustness across a wide range of non-uniform geometries and boundary conditions. Consistent agreement with independent semi-analytical and numerical benchmarks confirms the correctness of the proposed formulation, including cases where earlier studies reported inconsistent or physically questionable results. The analysis further confirms the existence and stability of the fundamental longitudinal mode for all well-posed boundary configurations. From a modal analysis perspective, the results reveal that smooth variations in cross-sectional geometry have a systematic influence on the distribution and sensitivity of natural frequencies. Higher vibration modes exhibit increased sensitivity to geometric variation and truncation order, while fixed–free configurations show greater numerical sensitivity compared to fixed–fixed and free–free cases. These trends are consistently captured by the proposed formulation.

Overall, the proposed differential transforms method provides a reliable, computationally efficient, and physically consistent framework for the modal analysis of non-uniform rods with smoothly varying geometries, offering clear advantages in terms of generality, numerical stability, and analytical transparency.

REFERENCES

1. Abrate, S. Vibration of non-uniform rods and beams. Journal of Sound and Vibration 1995; 185(4), 703–716. https://doi.org/10.1006/jsvi.1995.0410
2. Kumar, B.M., Sujith, R.I. Exact solutions for the longitudinal vibration of non-uniform rods. Journal of Sound and Vibration 1997; 207(5), 721–729.
3. Raj, A., Sujith, R.I. Closed-form solutions for the free longitudinal vibration of inhomogeneous rods. Journal of Sound and Vibration 2005; 283(3–5), 1015–1030. https://doi.org/10.1016/j.jsv.2004.06.003
4. Shuqi, G., Shaopu, Y. Free longitudinal vibrations of non-uniform rods. Science China Technological Sciences 2011; 54(10), 2735–2745. https://doi.org/10.1007/ s11431-011-4534-6

5. Rao S.S., Vibration of Continuous Systems, John Wiley & Sons, Hoboken, NJ, USA, 2007.
6. Reddy J.N., An Introduction to the Finite Element Method, 3rd ed., McGraw-Hill, New York, NY, USA, 2006.
7. Inman D.J., Engineering Vibration, 4th ed., Pearson Education, Upper Saddle River, NJ, USA, 2014.
8. Pukhov, G.E. Computational structure for solving differential equations by Taylor transformations. Cybernetics 1979; 14(3), 383–390. https://doi.org/10.1007/ BF01074670
9. Pukhov, G.E. Differential transforms and circuit-theory. International Journal of Circuit Theory and Applications 1982; 10(3), 265–276. https://doi.org/10.1002/cta.4490100307
10. Pukhov, G.E. Differential Transformations of Functions and Equations, 1980. http://catalog.lib.tpu.ru/catalogue/document/RU%255CTPU%255Cbook%255C211741
11. Pukhov, G.E. Differential Transformations and Mathematical Modeling of Physical Processes, 1986; 160.
12. Pukhov, G.E. Differential Spectrums and Models, 1990; 84.
13. Bervillier, C. Status of the differential transformation method. Applied Mathematics and Computation 2012; 218(20), 10158–10170. https://doi.org/10.1016/ j.amc.2012.03.094
14. Simonyan, S.H., Avetisyan, A.G. Applied Theory of Differential Transforms, 2010; 364. Chartaraget, Yerevan https://scholar.google.com/scholar?hl=en&as_sdt=0,5&cluster=14543917966785134975
15. Avetisyan, A.G., Simonyan, S.H., Ghazaryan, D.A. Solution of linear time opti-mal control problems in domain of differential transformations. Bulletin of Tomsk Polytechnical University 2009; 315(5), 5–13. https://earchive.tpu.ru/bitstream/11683/2920/1/bulletin_tpu-2009-315-5-42.pdf
16. Avetisyan, A.G., Avinyan, V.R., Ghazaryan, D.A. A method for solving Silvester type parametric matrix equation. Proceedings of the NAS RA and SEUA: Technical Sciences 2013; 66(4), 376–383.
17. Suddoung, K., Charoensuk, J., Wattanasakulpong, N. Application of the differential transformation method to vibration analysis of stepped beams with elastically constrained ends. Journal of Vibration and Control 2013; 19(16), 2387–2400. https://doi.org/10.1177/1077546312456581
18. Ebrahimi, F., Ghadiri, M., Salari, E., Hoseini, S.A.H., Shaghaghi, G.R. Application of the differential transformation method for nonlocal vibration analysis of functionally graded nanobeams. Journal of Mechanical Science and Technology 2015; 29(3), 1207–1215. https://doi.org/10.1007/s12206-015-0234-7
19. Ebrahimi, F., Mokhtari, M. Vibration analysis of spinning exponentially functionally graded Timoshenko beams based on differential transform method. Proceedings of the Institution of Mechanical Engineers, Part G: Journal of Aerospace Engineering 2015; 229(14), 2559–2571. https://doi.org/10.1177/0954410015580801
20. Ghazaryan, D., Burlayenko, V.N., Avetisyan, A., Bhaskar, A. Free vibration analysis of functionally graded beams with non-uniform cross-section using the differential transform method. Journal of Engineering Mathematics, 2018; 97–121. https://doi.org/10.1007/s10665-017-9937-3
21. Nourifar, M., Keyhani, A., Aftabi Sani, A. Free vibration analysis of rotating Euler–Bernoulli beam with exponentially varying cross-section by differential transform method. International Journal of Structural Stability and Dynamics, 2017; 1850024. https://doi.org/10.1142/S0219455418500244
22. Khosravi, A.E., Shahabian, F., Sani, A.A. Free vibration of cylindrical shells and panels with cutout via the differential transform method. Mechanics of Advanced Materials and Structures 2023. https://doi.org/10.1080/15376494.2023.2294494
23. Bozer, M. Ozarslan, M.A., Demez, H. Solutions of certain class of non-linear time-fractional diffusion equations via the fractional differential transform method. Miskolc Mathematical Notes 2023; 24. https://doi.org/10.18514/MMN
24. Bensabri, O., Hamza-Cherif, S.M., Mankour, A. Differential transformation method for free vibration analysis of an axially loaded overhung rotor. Inter-national Journal of Computational Materials Science and Engineering 2023. https://doi.org/10.1142/S2047684123500240
25. Khabiri, A., Javadi, A.S. Vibration analysis of buried pipelines and piles using differential transformation method. Proceedings of the Institution of Civil Engineers: Engineering and Computational Mechanics 2022; 175. https://doi.org/10.1680/jencm.21.00013
26. Suryaningrat, W., Anggriani, N., Supriatna, A.K. On application of differential transformation method to solve host-vector-predator system. In: Journal of Physics: Conference Series, 2021; 1722. https://doi.org/10.1088/1742-6596/ 1722/1/012040
27. Bozdo˘gan, K.B., Maleki, F.K. Application of differential transformation method for free vibration analysis of wind turbine. Wind and Structures, An International Journal 2021; 32. https://doi.org/10.12989/was.2021.32.1.011
28. He, Q., Tian, L., Qian, P., Tang, Z., Zhang, Z., Lu, T. Vibration characteristics analysis of the header assembly of combine harvester under multi-source coupled excitation. Agriculture 2025; 15, 2488. https://doi.org/10.3390/agriculture15232488

29. Nowakowski, M., Kosiuczenko, K. Evaluation of TAERO UGV structural collision resistance using FEM analysis. Bulletin of the Polish Academy of Sciences: Technical Sciences, 2025; 73(3), e153431. https://doi.org/10.24425/bpasts.2025.153431
30. Eisenberger, M. Exact Longitudinal Vibration Frequencies of a Variable Cross-Section Rod. Applied Acoustics 1991; 34, 123–130.
31. Leissa, A.W. The historical bases of the Rayleigh and Ritz methods. Journal of Sound and Vibration 2005; 287(4–5), 961–978. https://doi.org/10.1016/j.jsv.2004.12.021
32. Yardimoglu, B. Exact solutions for the longitudinal vibration of non-uniform rods [J. Sound Vib. 207, 721–729]. Journal of Sound and Vibration 1997; 329, 4107. https://doi.org/10.1016/j.jsv.2010.03.026
33. Sujith, R.I. Exact solutions for the longitudinal vibration of non-uniform rods: Author's reply. Journal of Sound and Vibration 2010; 329(19), 4108. https://doi.org/10.1016/j.jsv.2010.03.027
34. Elsaid, A. Fractional differential transform method combined with the Adomian polynomials. Applied Mathematics and Computation 2012; 218(12), 6899–6911. https://doi.org/10.1016/j.amc.2011.12.066